Received: 26 July 2020 | Revised: 2 October 2020 | Accepted: 20 October 2020

DOI: 10.1002/bit.27612

ARTICLE

BIOTECHNOLOGY AND BIOENGINEERING WILEY

Characterizing the effect of substrate stiffness on the extravasation potential of breast cancer cells using a 3D microfluidic model

Shohreh Azadi[1] | Mohammad Tafazzoli Shadpour[1] | Majid E. Warkiani[2,3]

[1]Faculty of Biomedical Engineering, Amirkabir University of Technology, Tehran, Iran

[2]School of Biomedical Engineering, University of Technology Sydney, Sydney, New South Wales, Australia

[3]Institute of Molecular Medicine, Sechenov University, Moscow, Russia

Correspondence
Mohammad Tafazzoli Shadpour, Faculty of Biomedical Engineering, AmirKabir University of Technology, Tehran 1591634311, Iran.
Email: tafazoli@aut.ac.ir

Abstract

Different biochemical and biomechanical cues from tumor microenvironment affect the extravasation of cancer cells to distant organs; among them, the mechanical signals are poorly understood. Although the effect of substrate stiffness on the primary migration of cancer cells has been previously probed, its role in regulating the extravasation ability of cancer cells is still vague. Herein, we used a microfluidic device to mimic the extravasation of tumor cells in a 3D microenvironment containing cancer cells, endothelial cells, and the biological matrix. The microfluidic-based extravasation model was utilized to probe the effect of substrate stiffness on the invasion ability of breast cancer cells. MCF7 and MDA-MB-231 cancer cells were cultured among substrates with different stiffness which followed by monitoring their extravasation capability through the microfluidic device. Our results demonstrated that acidic collagen at a concentration of 2.5 mg/ml promotes migration of cancer cells. Additionally, the substrate softening resulted in up to 46% reduction in the invasion of breast cancer cells. The substrate softening not only affected the number of extravasated cells but also reduced their migration distance up to 53%. We further investigated the secreted level of matrix metalloproteinase 9 (MMP9) and identified that there is a positive correlation between substrate stiffening, MMP9 concentration, and extravasation of cancer cells. These findings suggest that the substrate stiffness mediates the cancer cells extravasation in a microfluidic model. Changes in MMP9 level could be one of the possible underlying mechanisms which need more investigations to be addressed thoroughly.

KEYWORDS

collagen, extravasation, microfluidics, MMP9, substrate stiffness

1 | INTRODUCTION

Metastasis of primary tumor cells is responsible for more than 90% of cancer-related mortality (Jeon et al., 2013). The invasion of tumor cells is guided by a wide range of biochemical, biophysical, and genetic factors, making it a complex process (Jeon et al., 2015; Stuelten et al., 2018). Despite recent advancements in novel therapeutic strategies targeting the molecular pathways in tumor cells, the underlying mechanism of the metastasis cascade requires more investigations. Cancer progression is a multistep process that initiates from the formation of primary tumors and concluded with extravasation of cancer cells to second organs (Sokeland & Schumacher, 2019).

Extravasation is the last step before the formation of secondary tumor and plays a crucial role in cancer development and metastasis

(Ma et al., 2018). This step is influenced by a wide range of complex cellular and molecular interactions, as well as tumor microenvironmental (TME) cues which make it challenging to monitor and control the process (Ma et al., 2018). In this regard, several studies proposed the involvement of chemokine signals from the host organ (Bersini et al., 2014; Jeon et al., 2015; Xu et al., 2016), the interaction of cancer cells with endothelial and immune cells (Boussommier-Calleja et al., 2019; Lee et al., 2018), and biomechanical cues such as flow rate and shear stress (Polacheck et al., 2014), as well as physicomechanical properties of the extracellular matrix (ECM) of the host tissue (Wolf et al., 2013) in mediating the extravasation process. Before extravasation, tumor cells experience various TME chemical and mechanical cues which activate different cascades for structural and functional remodeling of cells (Emon et al., 2018). These cues further change the biological behavior of tumor cells and consequently their migration and invasion ability (Sleeboom et al., 2018). Such structural remodeling is mostly evident in altered cytoskeleton fiber content and arrangement, generation of traction forces, cell–cell and cell–ECM adherence, which all are determinants of cell motility (Paul et al., 2017). While numerous studies probed the effect of molecular and cellular interactions on the extravasation ability of cancer cells, the effect of previously experienced TME cues has not been deeply addressed yet.

Mechanical signals from the surrounding environment play a vital role in regulating tumor cell behavior (Chaudhuri et al., 2018; Emon et al., 2018). Specifically, in vitro studies have shown that tumor cell migration and motility are strongly affected by the substrate mechanics (Azadi, Tafazzoli-Shadpour, et al., 2019; van Helvert et al., 2018). Significant efforts have been spent on investigating the alteration of tumor cell structural and biological behavior in response to the rigidity of the cellular substrate such as change in cell morphology, adhesion, stiffness, protein expression, migration, and motility (Azadi, Tafazzoli-Shadpour, et al., 2019; Jiwlawat et al., 2019; Pandamooz et al., 2020; Rice et al., 2017a; Shukla et al., 2016). Despite the strong relationship between tumor invasiveness and ECM mechanics, the effect of ECM stiffness on the extravasation ability of tumor cells is still vague.

Investigating the underlying mechanism of the cellular invasion requires accurate modeling of TME. The microfluidic approach has been extensively utilized to provide a 3D microenvironment for modeling different steps of metastasis cascade (Ma et al., 2018; Osaki et al., 2018). A microfluidic platform containing three parallel channels has been developed to incorporate three main components of the extravasation process, including cancer cells, endothelial cells (ECs), and a biological matrix (Jeon et al., 2013). This model has demonstrated great potential in providing a physiologically relevant condition for tumor cells, and has been used by several research groups to probe the effect of different molecular signaling pathways on the extravasation of cancer cells (Chen et al., 2016; Jeon et al., 2015).

In this study, to mimic cancer cell remodeling induced by biomechanical cues, we engineered cells through cell–substrate interaction. The manipulated cells were introduced to a three-channel microfluidic device simulating extravasation to survey the effects of substrate mechanical properties on cancer cell invasion in a 3D microenvironment. The resulting model probes that the extravasation ability of cancer cells is affected by the characteristics which cancer cells achieved in response to different substrate stiffness. Our results can provide new insights into the complex mechanism underlying the extravasation stage of the metastasis cascade.

2 | MATERIALS AND METHODS

2.1 | Cell culture and substrate preparation

Two types of human breast cancer cell lines, MCF7 and MDA-MB-231, were acquired from the University of Technology Sydney. Cells were maintained in the RPMI culture medium (Thermo Fisher Scientific) containing 10% fetal bovine serum (FBS; Thermo Fisher Scientific) in an atmosphere of 5% CO_2 at 37°C. Human umbilical vein endothelial cells (HUVECs) were purchased from Lonza and cultured in EC growth basal medium-2 (EBM), supplemented with 10% FBS.

To examine whether the substrate stiffness affects the cellular invasion and extravasation, polydimethylsiloxane (PDMS) substrates with different stiffness values were utilized through mixing the silicone elastomer with the curing agent (Sylgard 184; Dow Corning) at three different ratios of 10:1 (stiff), 50:1 (semi-soft), and 75:1 (soft). The PDMS mixture was cured for 24 h at 70°C followed by coating with a thin layer of fibronectin (10 μg/ml; Sigma-Aldrich). Both types of cancer cells were cultured for 24 h among PDMS substrates with different stiffness, then detached and utilized for the cell migration and extravasation assays.

Cancer cells sense the surface properties of the substrate and respond to them at the micro level. While tensile testing provides the mechanical properties of bulk material, atomic force microscopy (AFM) nanoindentation method estimates the localized surface mechanical properties, which are sensed by cells. Therefore, the stiffness of PDMS substrates was measured using a NanoWizard2 AFM (JPK Instruments). V-shaped silicon nitride cantilever with a spring constant of 0.15 N/m^2 were utilized to indent the substrates at an approach velocity of 3 μm/s and a maximum indentation depth of 0.5 μm as previously described protocol (Azadi, Aboulkheyr, et al., 2019). The Young's modulus was estimated according to the modified Hertz model for a quadrilateral pyramid tip (Equation 1).

$$F(\delta) = \frac{1.49 E_{sub} \tan\alpha}{2(1-\vartheta_{sub}^2)}\delta^2 \quad (1)$$

where, F is the force, δ is the indentation depth, and α is the half-angle of pyramid tip which was set to 17.5°. The Poisson's ratio of substrates (ν_{sub}) was assumed to be 0.5 considering an incompressible material property for PDMS.

The substrates were examined at five random points from three independent experiments, which resulted in a total of 20 force-displacement curves for each substrate. The stiffness values of 1.1 ± 0.2 MPa, 14.3 ± 3.2 kPa, and 5.2 ± 1.3 kPa were obtained for the

stiff, semi-soft, and soft substrates, respectively. These values cover the physiologically relevant elastic moduli of TME that are used to examine how the substrate rigidity affects the biological behavior of cancer cells (Rianna & Radmacher, 2017; Staunton et al., 2016).

2.2 | Microfluidic system

To achieve a 3D model of cancer invasion and extravasation, a previously developed 3D microfluidic device was utilized (Jeon et al., 2013). The microfluidic devices were provided from AIM biotech to stimulate 3D migration and extravasation of cancer cells in a static condition. The microfluidic system contained three independently addressable parallel channels including a 1.3 mm-wide central channel and two 0.5 mm-wide side channels with 0.25 mm height. While the biological matrix was introduced to the central channel, cancer cells and ECs were added to the side channels to form a triple interaction between cancer cells, ECs, and ECM (Bersini et al., 2018).

Before conducting the extravasation assay, initial experiments were performed to find whether the collagen concentration, collagen pH, and the chemical stimulation affect the invasion ability of cancer cells. Initially, the collagen solution was prepared at a concentration of 2.5 mg/ml and pH 7.4 according to the previously published protocol and was injected to the central channel to represent ECM in 3D space (Chung et al., 2009; Jeon et al., 2013). The cancer cells were stained with Hoechst (1 μg/ml; Sigma-Aldrich) or PKH26 Red Fluorescent Cell tracker (10 μg/ml; Sigma-Aldrich) before loading to the device. The total number of 6×10^4 stained-cells in the serum-free media were injected to one of the side channels (cell channel), while the opposite channel was filled with the cell-free medium (media channel). The device incubated for one hour, followed by two times washing with culture media to remove any nonattached cells. Then, a chemoattractant gradient was created across the collagen gel by refilling the media channel with the FBS-enriched medium. This time point was considered as the starting point, and the migration of cancer cells was captured after 24 and 48 h using the fluorescent (IX73; Olympus), bright field (CKX53; Olympus), and Confocal microscopy (Ti; Nikon).

To find the effects of collagen concentration, collagen pH, and FBS stimulation, four study groups were defined for each cell line including control (collagen 2.5 mg, pH 7.4, with FBS gradient), acidic collagen (collagen 2.5 mg/ml, pH 6.5, with FBS gradient), dense collagen (collagen 3.5 mg/ml, pH 7.4, with FBS gradient), and without stimulation (collagen 2.5 mg, pH 7.4, without FBS gradient). Further, to evaluate how changes in collagen concentration and pH level affect the collagen architecture, the prepared hydrogels were captured using scanning electron microscopy (SEM; AIS2100; Seron Technologies).

2.3 | Invasion assay

To evaluate the effect of substrate stiffness on invasion of breast cancer cells, two configurations were used, which are named as "migration" and "extravasation." In migration configuration, cancer cells were seeded to the side channel in the absence of ECs. In contrast, in extravasation configuration, both endothelial and cancer cells were loaded to the side channel.

Before loading to the device, cancer cells were cultured among substrates with different stiffness to let them adapt to the micromechanical environment through structural remodeling. For the migration assay, the central channel was filled with collagen. Then, cancer cells were detached from substrates, centrifuged and stained with Hoechst. Then, the cell suspension was injected to one of the side channels in the presence of FBS stimulation. The migration of cancer cells was captured using fluorescent and/or confocal microscopy after 24 h. Analyzing the images showed that cancer cells migrated in the range of 0 μm (adhere to channel interface) to 300 μm. Therefore, the migrated area was divided into three zones from 0 to 100 μm as zone 1, 100–200 μm as zone 2, and 200–300 μm as zone 3.

In this paper, an accurate and physiologically relevant model of extravasation was presented similar to that described previously (Chen et al., 2016; Jeon et al., 2013). To achieve this model, a multistep process was followed as has been illustrated schematically in Figure 1. Briefly, first, the collagen solution was injected to the central channel. Then, HUVECs were detached, stained with Hoechst and loaded to the side channel with FBS-supplemented EBM medium at two concentrations of 1×10^6 and 1.5×10^6 cells/ml. They formed a confluent layer at the higher concentration within 24 h on the gel-media interface. In the next step, MCF7 and MDA-MB-231 cells were detached from stiff, semi-soft, and soft substrates followed by staining with CellTracker™ Green CMFDA Dye (1 μg/ml; Thermo Fisher Scientific). The stained cancer cells were injected to the endothelialized channel at the concentration of 0.5×10^5 cells/in the presence of FBS stimulation. The seeding density was chosen based on the previously published paper by Jeon et al. (2013) as the optimized seeding density of cancer cells to address both mimicking the low number of tumor cells of the in vivo condition and increasing the chance of extravasation event in each gel region. The transmigration of cancer cells across the endothelial layer into the collagen hydrogel was analyzed 24 h after loading the cancer cells.

2.4 | Permeability measurements

To confirm the integrity of a confluent EC layer, the diffusive permeability was assessed with fluorescently labeled dextran (70 kDa; Sigma-Aldrich) as the previously published protocol (Nagaraju et al., 2018). Two devices containing polymerized collagen in the central channel were used. While ECs were loaded to one device to form a confluent layer, the other device was used as a control without ECs. Upon the formation of a confluent EC layer, all media channels were aspirated. The cell-seeded side channel was re-filled with fluorescent dextran solution in culture medium at a concentration of 10 mg/ml, while the same volume of culture medium was injected to the opposite side channel to avoid any pressures difference. Both

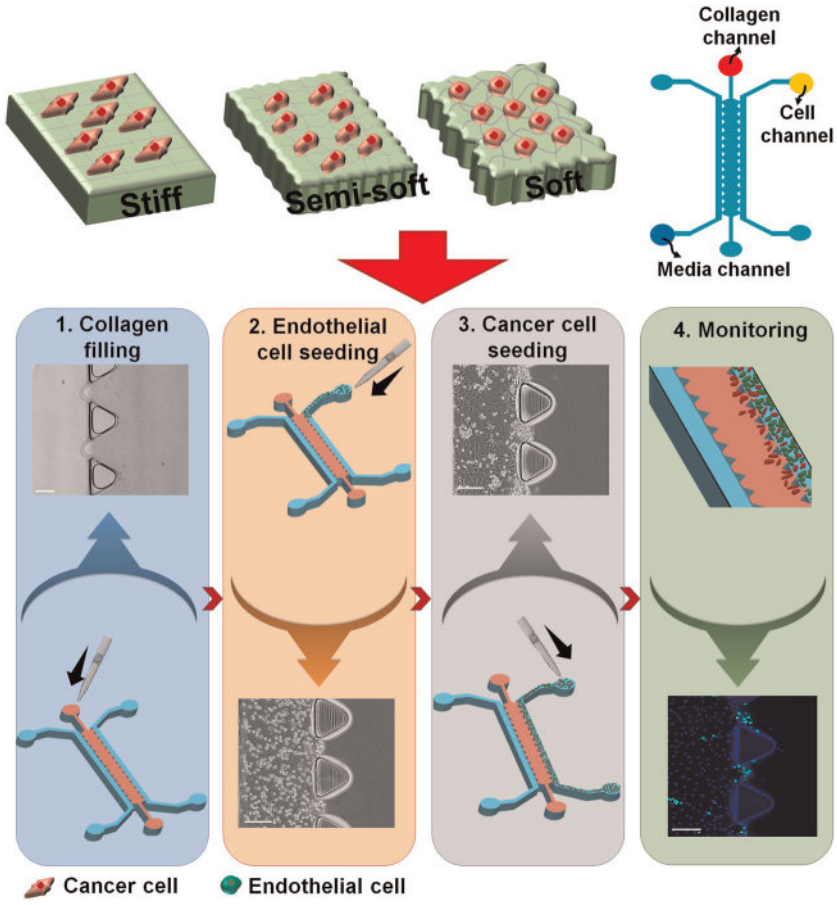

FIGURE 1 Schematic illustration of the workflow. Breast cancer cells were cultured among stiff, semi-soft, and soft substrates and assessed for their extravasation ability using a 3D microfluidic device. A multistep process was followed to incorporate collagen, endothelial cells (green), and cancer cells (red) into the target channels [Color figure can be viewed at wileyonlinelibrary.com]

microfluidic devices with and without EC layer were monitored, and images were captured using the fluorescent microscope immediately after injecting dextran. Then, devices were incubated for 1-h followed by imaging using fluorescent microscopy to find the dextran distribution in the collagen. The images were processed using ImageJ to obtain the fluorescent intensity and the permeability according to the previously described method (Vickerman & Kamm, 2012; Zervantonakis et al., 2012) based on the following equation:

$$P_D = D\left[\frac{(dc/dx)_{gel}}{\Delta C}\right], \quad (2)$$

where P_D is the diffusional permeability, ΔC is the concentration difference across the monolayer, D denotes the diffusion coefficient of dextran which was considered 4.5×10^{-11} m^2/s for 70 kDa dextran solution (Vickerman & Kamm, 2012), $(dC/dx)_{gel}$ is the concentration gradient of dextran in the gel region.

2.5 | Image analysis

All images were processed with ImageJ software. The particle analyzing feature was used for selecting and counting fluorescently labeled cells as well as finding the position of each migrated cell. For quantification purposes, a region of interest (ROI) with dimensions of 800 μm × 250 μm × 250 μm (height) was defined. The dimension of ROI was chosen to cover one gel-endothelial channel interface while considering all main components of extravasation, including cancer cells, ECs, and collagen. The chosen dimensions enabled quantifying the percentage of migrated cells in each ROI.

To find the effect of collagen concentration, collagen pH, and FBS stimulation, the total number of invaded cells and the average migrated distance were obtained from 30 to 40 ROIs of three independent devices per condition. The migration distance was calculated by considering the distance traveled by migrated cells from the gel-EC interface.

For both migration and extravasation assays, 48 ROIs from at least three independent devices were analyzed to find the percentage of extravasated cells and the invaded distance in each ROIs. The results were expressed as mean ± *SD* and compared using two-way analysis of variance (ANOVA) to find whether the substrate stiffening has a significant effect on each cell line. p-value < .05 was considered statistically significant.

2.6 | Evaluating the secretion of matrix metalloproteinase 9 (MMP9)

The secretion of MMP9 among different study groups of treated cells with varying substrate stiffness was examined by enzyme-linked

immunosorbent assay (ELISA). A SimpleStep ELISA kit (Abcam) was used according to the manufacturer's instruction. The optical density of samples was recorded at 450 nm to calculate the concentration of MMP9 protein in the samples. For each sample, three independent measurements were performed, and all the measurements were conducted in duplicate for statistical analysis.

3 | RESULTS

3.1 | Effects of collagen concentration and ph on the invasion of cancer cells

Figure 2a displays the migration of MDA-MB-231 cells toward collagen after 24 h of loading cancer cells to the side channel. Although the whole-device image confirmed that the migration of cancer cells is almost uniform in the whole channel, four ROIs close to the inlet and outlets were removed in data analyzing to avoid any nonuniformity resulted in 21 functional ROIs/device. Figure 2b displays a 3D image of the device using confocal microscopy, which confirms cancer cells migrated in different height of the gel, presenting a 3D microenvironment.

Figure 3 indicates how collagen density, pH, and chemical stimulation affect the migration of MCF7 and MDA-MB-231 cells in a 3D microenvironment. While representative fluorescent images have been shown in Figure 3a,b, the total number of invaded cells/device and the average migrated distance, have been presented in Figure 3c and 3d, respectively. By tracking the migrated cells over time, we explored the migration of cancer cells in two different time points of 24 and 48 h. The result demonstrated that the total number of migrated cells and the average migrated distance did not show a significant change from days 1 to 2 which suggests most migration events occur within the 1st day of loading cancer cells (t test, $p < .05$). This observation is consistent with previously reported in vitro and in vivo studies (Chen et al., 2013; Jeon et al., 2013).

As expected, in all study groups, MDA-MB-231 cells significantly showed a higher migration ability than MCF7 cells which confirms the dependency of tumor cell extravasation rate on their metastatic potential (Chen et al., 2013). Overall, the total number of invaded MDA-MB-231 cells was 3.5 times higher than MCF7 cells in control groups. Moreover, the average migrated distance of MDA-MB-231 cells was obtained 260 ± 34 μm which was significantly higher than the average migrated distance of 75 ± 10 μm for MCF7 cells in control groups (t test, $p < .05$; Figure 3c,d). Acidic microenvironment led to up to 44% and 27% increase in the number of invaded cells in MCF7, and MDA-MB-231 cell, respectively (t test, $p < .05$). Additionally, the migrated distance of cancer cells in acidic collagen

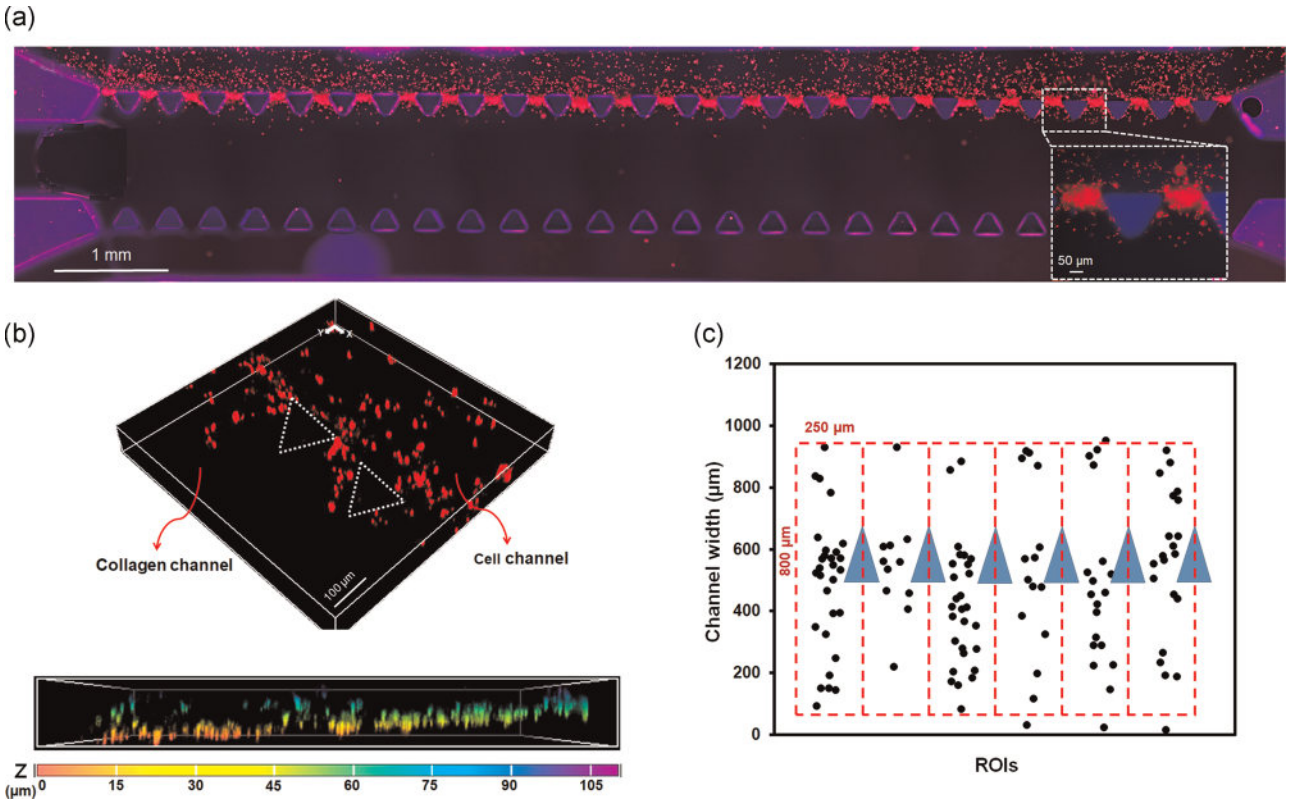

FIGURE 2 A 3D model of cancer cell migration on a microfluidic platform. (a) The representative whole-device image was captured by fluorescent microscope (IX73; Olympus) shows the migration of MDA-MB-231 cells toward collagen within 24 h. (b) The confocal images of cellular migration into the collagen confirms that cancer cells were surrounded by a 3D microenvironment as they were presented in different height of the collagen. (c) ROIs were defined as a region with dimension of 250 μm × 250 μm × 800 μm to incorporate EC layer, cancer cells, and gel region for data analysis. EC, endothelial cell; ROI, region of interest [Color figure can be viewed at wileyonlinelibrary.com]

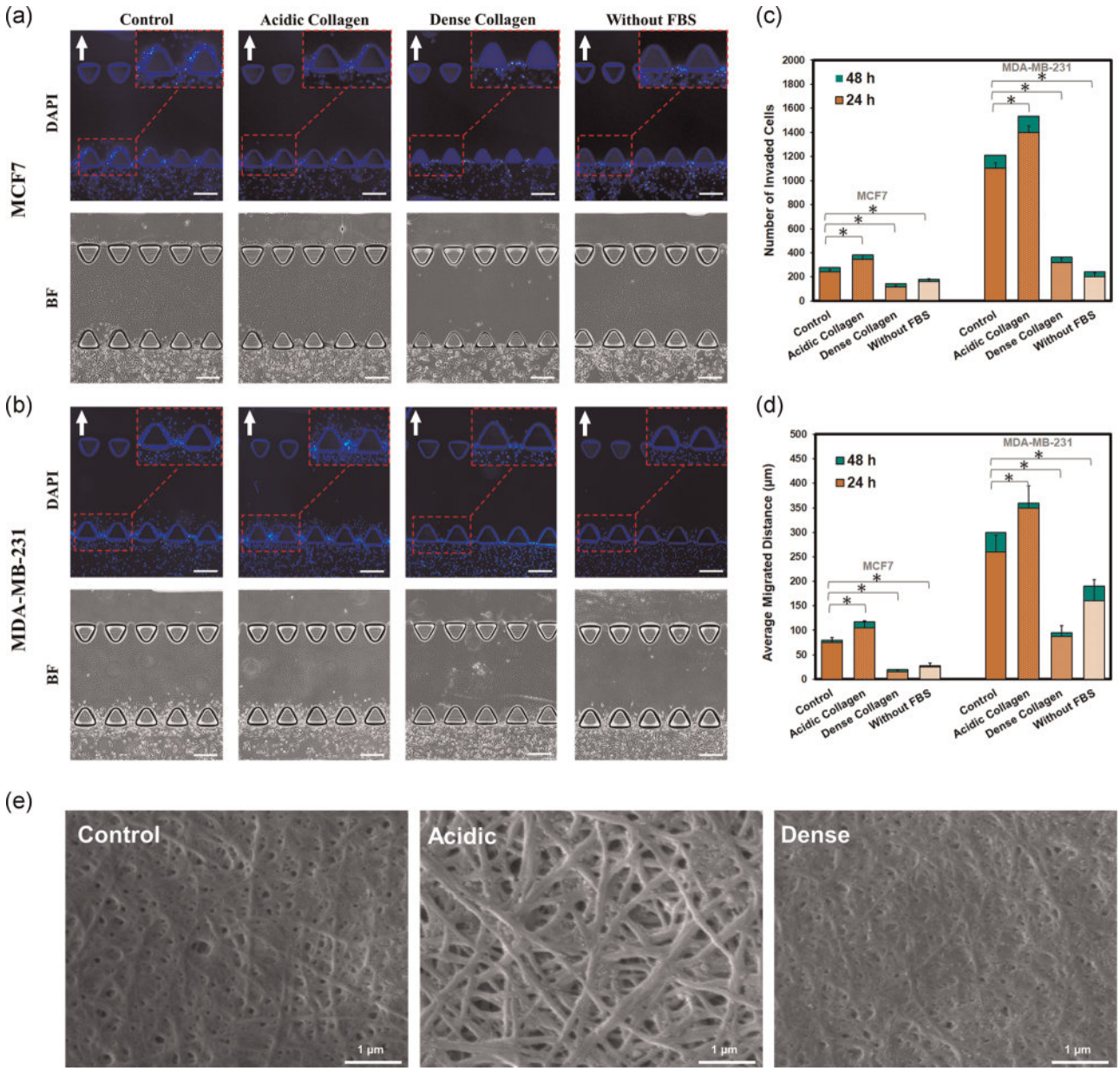

FIGURE 3 Evaluating the effect of collagen pH, collagen concentration, and FBS signaling on the invasion of breast cancer cells. Representative bright field and immunofluorescent images of (a) MCF7 and (b) MDA-MB-231 cells under different conditions of collagen concentration, pH, and FBS stimulation. Cancer cells were stained with Hoechst. The arrow indicates the direction of migration. Images were obtained using an inverted fluorescent microscope. The scale bar = 200 μm, and experiments were repeated three times. (c) Total number of invaded cells/device, and (d) average migrated distance in two different time points of 24 and 48 h among four study groups of MCF7 and MDA-MB-231 cells. (e) Representative SEM images of collagen in control (2.5 mg/ml, pH 7.4), acidic (2.5 mg/ml, pH 6.5), and dense (3.5 mg/ml, pH 7.4) groups, scale bar = 1 μm. *Indicate the significant differences at time point of 24 h (*t* test, $p < .05$). FBS, fetal bovine serum; SEM, scanning electron microscopy [Color figure can be viewed at wileyonlinelibrary.com]

considerably changed from 75 ± 10 μm to 105 ± 14 μm for MCF7 cells, and from 260 ± 34 μm to 350 ± 45 μm for MDA-MB-231 cells (*t* test, $p < .05$).

Figure 3e indicates that the morphology of collagen network and its porosity are highly affected by pH. The collagen microstructure appeared tighter at higher pH while decreasing the pH resulted in thicker collagen fibers. Furthermore, SEM images displayed that ECM morphology was affected not only by pH, but also by collagen concentration. Tighter networks were formed by increasing collagen concentration. Several studies have pointed out the similar effect of pH and concentration on mechanical properties and microstructure of the collagen hydrogels (Achilli & Mantovani, 2010; Anguiano et al., 2017). Both cancer cells exhibited a significant decrease in the migration ability by changing the collagen concentration from 2.5 to 3.5 mg/ml (Figure 3). Such reduction was obtained 52% and 243% in the number of invaded MCF7 and MDA-MB-231 cells, respectively,

which highlights the vital role of the collagen concentration in the invasion of cancer cells. Additionally, cancer cells exhibited a lower penetration distance in 3D dense collagen compared to samples with normal collagen concentration.

Usually, cancer cells migrate to distant organs following chemical gradients (Nguyen et al., 2009). Here, we used FBS-enriched media to simulate the migration of cancer cells in a TME. FBS-supplemented media in the opposite channel successfully triggered the migration of breast cancer cells (Figure 3c,d), most intensely in MDA-MB-231 cells. Based on the obtained results, further migration and extravasation experiments were defined with collagen at concentration of 2.5 mg/ml, pH 7.4, under FBS-stimulated condition, which resulted in a significant number of extravasation events.

3.2 | Microfluidic-based 3D migration assay

3D migration of MCF7 and MDA-MB-231 cells, manipulated by culturing on stiff, semi-soft, and soft substrates, has been shown in Figure 4. While Figure 4a displays the representative fluorescent and bright-field images of cellular migration among study groups, the quantitative analyses are reported in Figure 4b–f. The results obtained after 24 h of loading cancer cells to the device demonstrate that the cellular migration strongly depends on the stiffness of the initial cellular substrates. Both types of breast cancer cells derived from the stiff substrates exhibited a higher migration ability compared to those derived from the soft substrates (Figure 4e,f, two-way ANOVA, $p < .05$). Analyzing the images in three different zones of 0–100, 100–200, and 200-300 μm enabled the quantification of

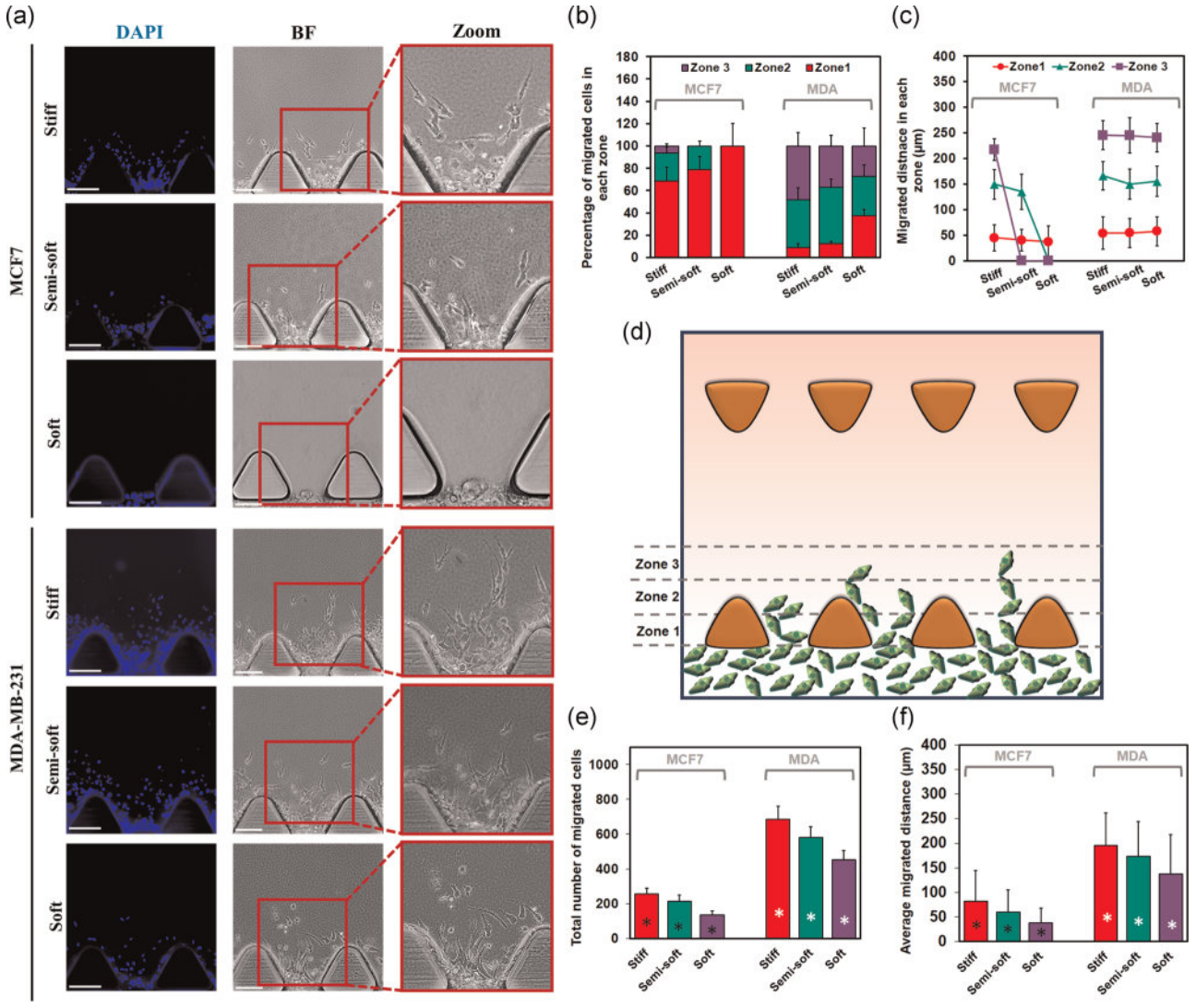

FIGURE 4 3D migration of breast cancer cells derived from stiff, semi-soft, and soft substrates in a microfluidic device. (a) Representative fluorescent and BF images of cellular migration among study groups with scale bar = 100 μm. (b) Percentage of migrated cells in three different zones. (c) Average migrated distance in each zone. (d) Schematic illustration of zone 1, 2, and 3 with a width of 100 μm in a microfluidic device. (e) Total number of migrated cells (*two-way ANOVA, $p < .05$). (f) Average migrated distance among stiff, semi-soft, and soft groups of MCF7 and MDA-MB-231 cells (*two-way ANOVA, $p < .05$). ANOVA, analysis of variance; BF, bright-field [Color figure can be viewed at wileyonlinelibrary.com]

cellular migration. The percentage of migrated cells and the average migrated distance in each zone have been reported in Figure 4b,c, which resulted in a better comparison of the migration ability of cancer cells. Moreover, the total number of invaded cells and the average migrated distance have been reported in Figure 4e,f.

Results demonstrate that substrate softening significantly increased the percentage of migrated cells in zone 1 for both MCF7 and MDA-MB-231 cells (Figure 4b), while decreased the migrated cells in zone 2, and 3. Noninvasive MCF7 cells did not migrate to zone 3 in semi-soft and soft groups which confirms their lower migration ability on the soft substrates. This behavior resulted in 46.8% and 54.2% reduction in the total number of migrated cells and average migrated distance of MCF7 by substrate softening, respectively, as shown in Figure 4e,f. On the other hand, MDA-MB-231 cells migrated to all three zones in stiff, semi-soft, and soft groups with different ratios. For example, 8.76%, 43.23%, and 48% of MDA-MB-231 cells in the stiff group migrated to zone 1, 2, and 3, respectively, while these values changed to 37.35%, 35.15%, and 27.5% in the soft group, correspondingly. Overall, Figure 4e,f indicate that substrate stiffening led to 52% and 42% increase in the total number of migrated MDA-MB-231 cells and their average migrated distance, respectively. Statistical analysis using two-way ANOVA demonstrated that there is a significant correlation between substrate stiffening and cancer cell migration in terms of both the migration percentage and the migrated distance ($p < .05$).

To assess the morphology of migratory cells, their shape index was measured using ImageJ which is defined as $SI=4\pi A/p^2$, where A is the projected area, and p is the cell perimeter (Rueden et al., 2017). SI was reported as mean ± SD by averaging the SI values of at least ten different cells from each group of study in Figure 4a. The shape indices of 0.36 ± 0.19, 0.42 ± 0.12, and 0.67 ± 0.21 were obtained for MCF7 migratory cells in stiff, semi-soft, and soft groups, respectively, while the SI values of 0.15 ± 0.07, 0.28 ± 0.09, and 0.27 ± 0.15 were calculated for MDA-MB-231 cells in stiff, semi-soft, and soft groups, respectively. This result indicates that those cells originated from stiff substrates could be elongated more than cells originated from soft substrates, which resulted in lower shape index (two-way ANOVA, $p < .05$). These morphological changes further promoted the migration of cancer cells.

3.3 | Assessing the integrity of EC layer

The integrity of EC layer was assessed firstly using bright field and fluorescent microscopy at two different seeding concentrations as shown in Figure 5a, and further confirmed through permeability measurements in Figure 5b,c. HUVECs labeled with cell tracker and Hoechst formed a confluent layer 1 day after cell seeding at concentration of 1.5 million cells/ml but not at concentration of 1 million cells/ml (Figure 5a). The permeability measurements further confirmed the integrity of the formed endothelial layer at the higher concentration. Quantifying the permeability measurement in Figure 5c confirmed that the dextran diffusion into the collagen had been significantly limited in the ECs-containing device. The device containing collagen and endothelial layer exhibited considerably lower permeability compared to the control device containing collagen without ECs (Figure 5b,c). The diffusional permeability of 0.45×10^{-6} cm/s was calculated for 70 kDa Dextran, which is in good agreement with previously reported values (Vickerman & Kamm, 2012; Zervantonakis et al., 2012).

3.4 | Modeling the extravasation of cancer cells

Figure 6 indicates that the extravasation of breast cancer cells is affected by the substrate stiffness. While ECs were stained with Hoechst, cancer cells labeled with green cell tracker before loading to the endothelial channel. Then, cancer cells transmigrated through endothelial junctions and entered to the collagen channel (Figure 6a). The extravasated MCF7 and MDA-MB-231 cells derived from three different stiff, semi-soft, and soft substrates were quantified in terms of percentage of invaded cells and the extravasated distance after 24 h (Figure 6b,c). Comparison of Figures 4 and 6 indicates that the endothelial layer considerably limited the invasion of cancer cells. Cancer cells showed 50% reduction in the invasion in the presence of ECs which is consistent with previously published papers (Zhang et al., 2012). This result further confirms the formation of an integrated endothelial layer.

Substrate stiffness significantly affected the extravasation of invasive cancer cells (two-way ANOVA, $p < .05$) but not the noninvasive cancer cells. The percentage of extravasated MDA-MB-231 cells decreased from 40 ± 12% in the stiff group to 36 ± 12.5% in semi-soft, and 30 ± 6.87% in the soft groups. The extravasation percentage of noninvasive MCF7 cells was decreased from 16.75 ± 4% in the stiff group to 13.27 ± 3.51% and 14.5 ± 5.21% in the semi-soft and soft groups, respectively (Figure 6c). Since the invaded cells located in different positions in the range of 0–145 μm, we used box plot to report the range of migrated distance and its median (Figure 6b), however, the average migrated distance also exhibited a significant reduction by substrate softening ($p < .05$).

3.5 | Alteration of MMP9 secretion of cancer cells in response to the substrate stiffening

To further investigate how the substrate stiffening can affect the invasion of breast cancer cells, MMP9 secretion of cancer cells was measured among three study groups. MMP9 is secreted by cancer cells and plays an important role in the breakdown of ECM through degrading ECM fibers. Our results in Figure 6d indicate that MMP9 secretion was highly affected by the substrate stiffness (two-way ANOVA, $p < .05$). The concentration of secreted MMP9 of MDA-MB-231 cells was obtained 502.6 ± 17.5 pg/ml in the stiff group and decreased to the 452 ± 33 pg/ml and 152.74 ± 3.87 pg/ml in the semi-soft and soft groups, respectively. Overall, MMP9 secretion of MCF7 cells in all three study groups was significantly lower than MDA-MB-231 cells which is

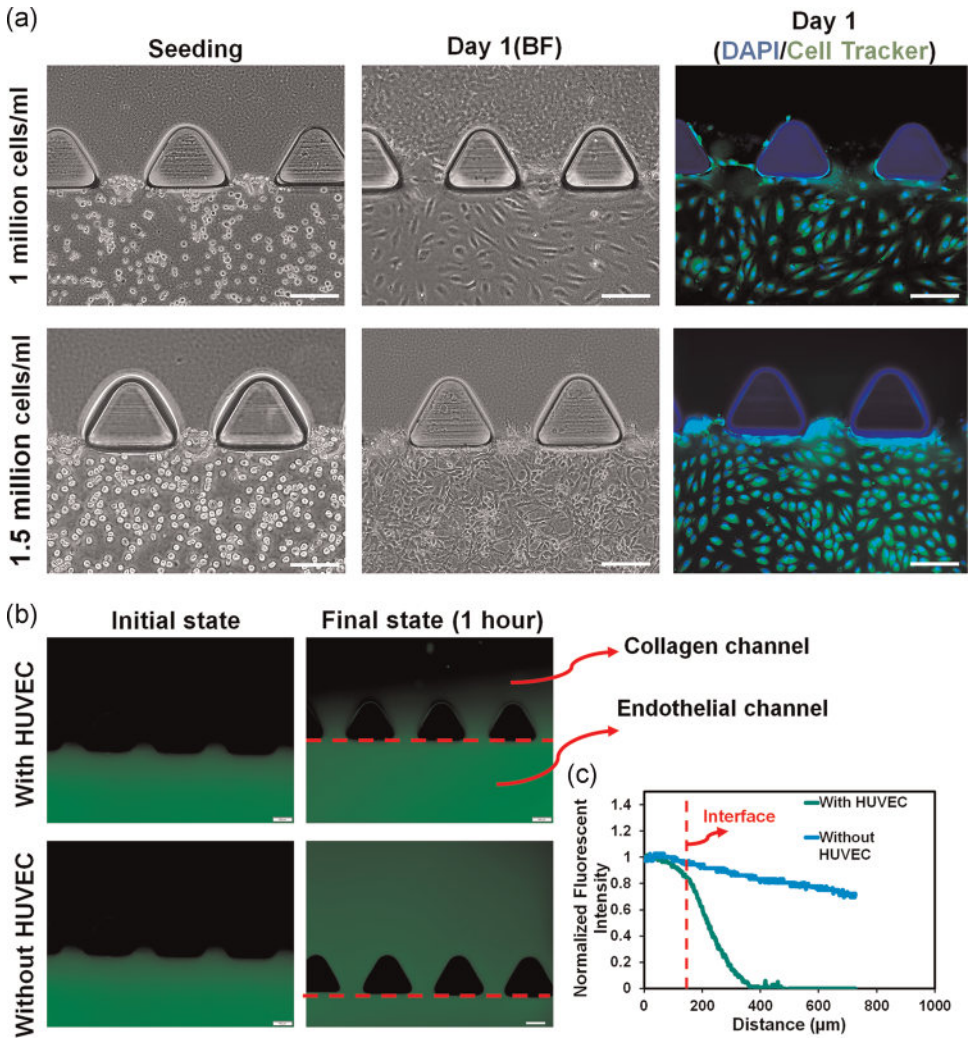

FIGURE 5 Assessing the integrity of endothelial layer. (a) Representative bright field and fluorescent images of endothelial cells labeled with cell tracker and Hoechst at two different seeding concentrations. (b) Fluorescent images of dextran diffusion in the microfluidic device containing collagen with/without endothelial cells, scale bar = 100 μm. (c) Normalized fluorescent intensity across a ROI obtained using ImageJ. ROI, region of interest [Color figure can be viewed at wileyonlinelibrary.com]

consistent with their noninvasive phenotype. Moreover, the MMP9 concentration of 94 ± 4.2 pg/ml for MCF7 cells in the stiff group showed 35.2% reduction in the soft group and reached to the value of 62 ± 7.5 pg/ml (Figure 6d).

4 | DISCUSSION

Biochemical composition, mechanical stimuli, and cellular components of TME play pivotal roles in cancer progression, among which, mechanical features are gaining significant attention in recent years (Emon et al., 2018; Sleeboom et al., 2018). Mechanical features of TME have been generally investigated in terms of ECM stiffness (Najafi et al., 2019), fiber alignment (Ray et al., 2017), and porosity (Blackmon et al., 2016). It is well established that cancer cells change the signaling pathways, protein expressions, proliferation, and differentiation in response to these mechanical cues (Sleeboom et al., 2018; Walker et al., 2018). To the best of our knowledge, no research has been reported whether substrate stiffness affects the migratory behavior of cancer cells in the late stages of the metastasis cascade including extravasation.

Cellular behaviors such as migration and motility are highly affected by the substrate stiffness during in vitro culture. Our results indicate that, interestingly, even for invasive cancer cells that already underwent structural deformations due to cancer-related alterations, they further remodeled in response to the substrate stiffness. This observation confirms that both noninvasive and invasive cancer cells respond to the mechanical changes of the surrounding environment.

Our results further confirmed that the invasion of cancer cells into the 3D collagen is closely related to the structural features of the collagen, including porosity and fiber thickness. It is expected that the collagen stiffness is increased by increasing the collagen concentration, as previously reported (Wullkopf et al., 2018). This observation is most likely due to thicker fibers and smaller pore

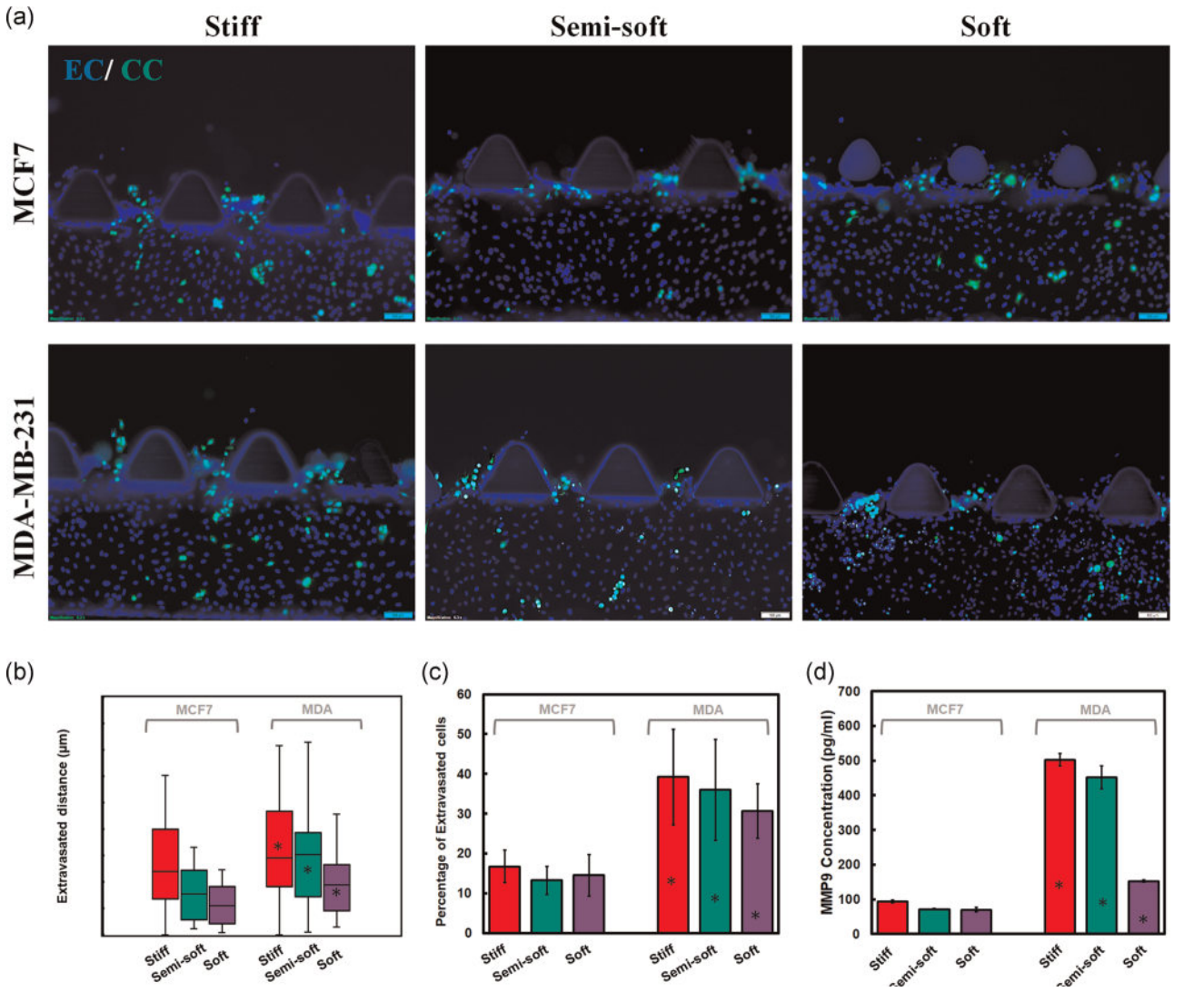

FIGURE 6 Extravasation of breast cancer cells among three study groups of stiff, semi-soft, and soft substrates. (a) Representative fluorescent images of extravasation of MCF7 and MDA-MB-231 cells among three substrates, while ECs were stained with Hoechst (blue) and CCs, were labeled with green cell tracker, the scale bar = 100 μm. (b) The invaded distance of cancer cells. (c) The percentage of extravasation of MCF7 and MDA-MB-231 cells. (d) Concentration of MMP9 among study groups of MCF7 and MDA-MB-231 cells measured by ELISA. The results were compared using ANOVA two-way, $p < .05$. ANOVA, analysis of variance; CC, cancer cell; EC, endothelial cell; ELISA, enzyme-linked immunosorbent assay; MMP, matrix metalloproteinase [Color figure can be viewed at wileyonlinelibrary.com]

sizes (Figure 3e). Several studies highlighted that different parameters, including the cross-linking method, collagen concentration, temperature, and pH affect the mechanical properties of collagen hydrogels (Achilli & Mantovani, 2010; Anguiano et al., 2017). Here, we used a physical cross-linking method to avoid adding any extra chemical agent which could affect the viability of cells and other cellular behaviors such as motility. The SEM images showed that both collagen concentration and pH altered collagen microstructure in terms of fiber thickness and tightening, which consequently affect the collagen stiffness (Lang et al., 2015; Wolf et al., 2013).

Decreased pH is a common characteristic of tumor ECM compared to the normal matrix, which influences cancer cell behaviors, proliferation, metastasis, and tumorigenesis (White et al., 2017). Our results showed that cancer cells highly invaded into the collagen with lower pH. Brown and Murray (2015) reported that decreased pH enables cell invasion by increasing the activity of acid-activated MMPs. Interestingly, not only the number of migrated cells but also their migrated distance increased in the acidic environment. This observation could be due to changes in the collagen microstructure through increasing fiber thickness and decreasing fiber tightening upon a decrease in pH, which facilitated the migration of cancer cells. Moreover, a higher concentration of collagen resulted in tighter collagen network with thinner fibers which consequently decreased the invasion of cancer cells into the collagen. In this regard, Wolf et al., (2013) studied the migration of cancer cells within 3D collagen with different stiffness values and observed that migration speed increased with decreasing collagen concentration due to change in pore sizes.

The presented model of cancer cell invasion exhibited the elongated morphology of invaded cells with cell protrusions into the 3D collagen (Figure 4a). Specifically, invasive MDA-MB-231 cancer cells exhibited more elongations up to 100 μm compared to MCF7 cells. Moreover, invaded cells showed a clear alignment in the chemical gradient direction. This morphology could be due to the transmigration through narrow endothelial junctions. Chen et al. (2013) previously described this behavior by visualizing the extravasation of cancer cells in a vascularized microenvironment. Figure 4 also probed that cancer cell migration occurs in the form of the cellular aggregates while one cell is moving as the leader. This specific behavior has been described previously (Zhang et al., 2012). Zhang et al. reported that the invasion ability of cellular aggregates is more than individual cells, and they prefer to move as cancer cell clusters (Au et al., 2016).

Changes in the extravasation of cancer cells in response to substrate stiffness can be related to alterations in different cellular and molecular signaling pathways. More specifically, substrate stiffness affects epithelial to mesenchymal transition (EMT), which may consequently modulate the migration and metastasis of cancer cells (Dong et al., 2019; Matte et al., 2019). It has been demonstrated that hypoxia and stiffer substrate synergistically induce EMT of MCF7 cells (Lv et al., 2017). Similar findings suggested the highest level of vimentin and the lowest level of E-cadherin in cancer cells cultured on stiff substrates (Piao et al., 2017). These changes were accompanied with changes in cell shape toward a mesenchymal phenotype along with increased migration of cancer cells cultured on stiff substrates (Dong et al., 2019; Matte et al., 2019; Rice et al., 2017). All these findings suggest that the relation between substrate stiffness and the extravasation potential can be associated with changes in cellular phenotype.

MMP9, as one of the most significant proteases during cancer progression, plays an essential role in cleaving many ECM proteins (Huang, 2018). Previous studies highlighted a positive correlation between substrate stiffness and MMP9 expression which could affect the invasion behavior of cells (Zhao, Li, et al., 2018; Zhao, Xue, et al., 2018). It has been demonstrated that MMP9 expression and activity is associated with the invasion of cancer cells. For example, downregulation of MMP9 through knockdown of E-26 transformation-specific-1 (Ets-1) in MCF7 and MDA-MB-231 cells resulted in reduced cell invasion and altered expression of EMT markers (Nazir et al., 2019).

Additionally, it has been shown that increased expression of MMP9 in MCF7 cells resulted in invasion of cells, while the reduced invasion of MDA-MB-231 cells was observed upon downregulation of MMP9 (Gil et al., 2016). More recently, it was demonstrated that MMP9 promotes colonization of circulating tumor cells into the lungs, while blocking MMP9 signaling inhibited experimental lung metastases (Owyong et al., 2019). All these findings demonstrates the association between MMP9 expression level/activity and cancer cell invasion. Both types of cancer cells decreased the secretion of MMP9 on the soft substrates (Figure 6d) which can be one of the possible underlying mechanism for the lower invasion ability of these cells during the extravasation step.

In conclusion, the presented microfluidic-based extravasation model revealed that cancer cells noticeably increase their extravasation ability in response to the substrate stiffening which could be correlated with the expression level of MMP9. TME cues, either chemical or mechanical, play a remarkable role in modulating the behavior of cancer cells and the state of cancer progress. Considering this vital role opens a different point of view to cancer treatment approaches which include both directly targeting cancer cells and/or pointing TME features. One of the limitations of the current study is related to the lack of a long-term culture of cancer cells in the microfluidic device. The long-term culture will provide the possibility of examining the colonization of cancer cells. Such study can be useful in probing the effect of ECM stiffness in the formation of the secondary tumors, however, most likely it requires re-engineering of the microfluidic model which remains an interesting topic for the future research.

CONFLICT OF INTERESTS

The authors declare that they have no conflict of interests.

AUTHOR CONTRIBUTIONS

Shohreh Azadi carried out the experiments and wrote the manuscript. Majid E. Warkiani contributed in designing the experiments and analysis the results. Mohammad Tafazzoli Shadpour supervised the project and helped to analyze the results and edit the manuscript.

ORCID

Mohammad Tafazzoli Shadpour http://orcid.org/0000-0001-5387-8632

REFERENCES

Achilli, M., & Mantovani, D. (2010). Tailoring mechanical properties of collagen-based scaffolds for vascular tissue engineering: The effects of pH, temperature and ionic strength on gelation. *Polymers*, *2*(4), 664–680. https://doi.org/10.3390/polym2040664

Anguiano, M., Castilla, C., Maška, M., Ederra, C., Peláez, R., Morales, X., Muñoz-Arrieta, G., Mujika, M., Kozubek, M., Muñoz-Barrutia, A., Rouzaut, A., Arana, S., Garcia-Aznar, J. M., & Ortiz-de-Solorzano, C. (2017). Characterization of three-dimensional cancer cell migration in mixed collagen-Matrigel scaffolds using microfluidics and image analysis. *PLOS One*, *12*(2), e0171417. https://doi.org/10.1371/journal.pone.0171417

Au, S. H., Storey, B. D., Moore, J. C., Tang, Q., Chen, Y. L., Javaid, S., Sarioglu, A. F., Sullivan, R., Madden, M. W., O'Keefe, R., Haber, D. A., Maheswaran, S., Langenau, D. M., Stott, S. L., & Toner, M. (2016). Clusters of circulating tumor cells traverse capillary-sized vessels. *Proceedings of the National Academy of Sciences of the United States of America*, *113*(18), 4947–4952. https://doi.org/10.1073/pnas.1524448113

Azadi, S., Aboulkheyr, E. S. H., Razavi Bazaz, S., Thiery, J. P., Asadnia, M., Ebrahimi, & Warkiani, M. (2019). Upregulation of PD-L1 expression in breast cancer cells through the formation of 3D multicellular cancer aggregates under different chemical and mechanical conditions. *Biochimica et Biophysica Acta (BBA)-Molecular Cell Research*, *1866*(12), 118526. https://doi.org/10.1016/j.bbamcr.2019.118526

Azadi, S., Tafazzoli-Shadpour, M., Soleimani, M., & Warkiani, M. E. (2019). Modulating cancer cell mechanics and actin cytoskeleton structure by chemical and mechanical stimulations. *Journal of Biomedical Materials Research, Part A*, *107*(8), 1569–1581. https://doi.org/10.1002/jbm.a.36670

Bersini, S., Jeon, J. S., Dubini, G., Arrigoni, C., Chung, S., Charest, J. L., Moretti, M., & Kamm, R. D. (2014). A microfluidic 3D in vitro model for specificity of breast cancer metastasis to bone. *Biomaterials*, *35*(8), 2454–2461. https://doi.org/10.1016/j.biomaterials.2013.11.050

Bersini, S., Miermont, A., Pavesi, A., Kamm, R. D., Thiery, J. P., Moretti, M., & Adriani, G. (2018). A combined microfluidic-transcriptomic approach to characterize the extravasation potential of cancer cells. *Oncotarget*, *9*(90), 36110–36125. https://doi.org/10.18632/oncotarget.26306

Blackmon, R. L., Sandhu, R., Chapman, B. S., Casbas-Hernandez, P., Tracy, J. B., Troester, M. A., & Oldenburg, A. L. (2016). Imaging extracellular matrix remodeling in vitro by diffusion-sensitive optical coherence tomography. *Biophysical Journal*, *110*(8), 1858–1868. https://doi.org/10.1016/j.bpj.2016.03.014

Boussommier-Calleja, A., Atiyas, Y., Haase, K., Headley, M., Lewis, C., & Kamm, R. D. (2019). The effects of monocytes on tumor cell extravasation in a 3D vascularized microfluidic model. *Biomaterials*, *198*, 180–193. https://doi.org/10.1016/j.biomaterials.2018.03.005

Brown, G. T., & Murray, G. I. (2015). Current mechanistic insights into the roles of matrix metalloproteinases in tumour invasion and metastasis. *The Journal of Pathology*, *237*(3), 273–281. https://doi.org/10.1002/path.4586

Chaudhuri, P. K., Low, B. C., & Lim, C. T. (2018). Mechanobiology of tumor growth. *Chemical Reviews*, *118*(14), 6499–6515. https://doi.org/10.1021/acs.chemrev.8b00042

Chen, M. B., Lamar, J. M., Li, R., Hynes, R. O., & Kamm, R. D. (2016). Elucidation of the roles of tumor integrin β1 in the extravasation stage of the metastasis cascade. *Cancer Research*, *76*(9), 2513–2524.

Chen, M. B., Whisler, J. A., Jeon, J. S., & Kamm, R. D. (2013). Mechanisms of tumor cell extravasation in an in vitro microvascular network platform. *Integrative Biology*, *5*(10), 1262–1271. https://doi.org/10.1039/c3ib40149a

Chung, S., Sudo, R., Mack, P. J., Wan, C. R., Vickerman, V., & Kamm, R. D. (2009). Cell migration into scaffolds under co-culture conditions in a microfluidic platform. *Lab on a Chip*, *9*(2), 269–275. https://doi.org/10.1039/b807585a

Dong, Y., Zheng, Q., Wang, Z., Lin, X., You, Y., Wu, S., Wang, Y., Hu, C., Xie, X., Chen, J., Gao, D., Zhao, Y., Wu, W., Liu, Y., Ren, Z., Chen, R., & Cui, J. (2019). Higher matrix stiffness as an independent initiator triggers epithelial-mesenchymal transition and facilitates HCC metastasis. *Journal of Hematology & Oncology*, *12*(1), 112.

Emon, B., Bauer, J., Jain, Y., Jung, B., & Saif, T. (2018). Biophysics of tumor microenvironment and cancer metastasis—A mini review. *Computational and Structural Biotechnology Journal*, *16*, 279–287. https://doi.org/10.1016/j.csbj.2018.07.003

Gil, M., Kim, Y. K., Kim, K.-E., Kim, W., Park, C.-S., & Lee, K. J. (2016). Cellular prion protein regulates invasion and migration of breast cancer cells through MMP-9 activity. *Biochemical and Biophysical Research Communications*, *470*(1), 213–219.

van Helvert, S., Storm, C., & Friedl, P. (2018). Mechanoreciprocity in cell migration. *Nature Cell Biology*, *20*(1), 8–20. https://doi.org/10.1038/s41556-017-0012-0

Huang, H. (2018). Matrix metalloproteinase-9 (MMP-9) as a cancer biomarker and MMP-9 biosensors: Recent advances. *Sensors*, *18*(10), 3249. https://doi.org/10.3390/s18103249

Jeon, J. S., Bersini, S., Gilardi, M., Dubini, G., Charest, J. L., Moretti, M., & Kamm, R. D. (2015). Human 3D vascularized organotypic microfluidic assays to study breast cancer cell extravasation. *Proceedings of the National Academy of Sciences of the United States of America*, *112*(1), 214–219. https://doi.org/10.1073/pnas.1417115112

Jeon, J. S., Zervantonakis, I. K., Chung, S., Kamm, R. D., & Charest, J. L. (2013). In vitro model of tumor cell extravasation. *PLOS One*, *8*(2), e56910. https://doi.org/10.1371/journal.pone.0056910

Jiwlawat, N., Lynch, E. M., Napiwocki, B. N., Stempien, A., Ashton, R. S., Kamp, T. J., Crone, W. C., & Suzuki, M. (2019). Micropatterned substrates with physiological stiffness promote cell maturation and Pompe disease phenotype in human induced pluripotent stem cell-derived skeletal myocytes. *Biotechnology and Bioengineering*, *116*(9), 2377–2392.

Lang, N. R., Skodzek, K., Hurst, S., Mainka, A., Steinwachs, J., Schneider, J., Aifantis, K. E., & Fabry, B. (2015). Biphasic response of cell invasion to matrix stiffness in three-dimensional biopolymer networks. *Acta Biomaterialia*, *13*, 61–67. https://doi.org/10.1016/j.actbio.2014.11.003

Lee, S. W. L., Adriani, G., Ceccarello, E., Pavesi, A., Tan, A. T., Bertoletti, A., Kamm, R. D., & Wong, S. C. (2018). Characterizing the role of monocytes in T cell cancer immunotherapy using a 3D microfluidic model. *Frontiers in Immunology*, *9*, 416.

Lv, Y., Chen, C., Zhao, B., & Zhang, X. (2017). Regulation of matrix stiffness on the epithelial-mesenchymal transition of breast cancer cells under hypoxia environment. *The Science of Nature*, *104*(5-6), 38.

Ma, Y. H. V., Middleton, K., You, L. D., & Sun, Y. (2018). A review of microfluidic approaches for investigating cancer extravasation during metastasis. *Microsystems & Nanoengineering*, *4*, 17104. https://doi.org/10.1038/micronano.2017.104

Matte, B. F., Kumar, A., Placone, J. K., Zanella, V. G., Martins, M. D., Engler, A. J., & Lamers, M. L. (2019). Matrix stiffness mechanically conditions EMT and migratory behavior of oral squamous cell carcinoma. *Journal of Cell Science*, *132*(1), jcs224360.

Nagaraju, S., Truong, D., Mouneimne, G., & Nikkhah, M. J. (2018). Microfluidic tumor–vascular model to study breast cancer cell invasion and intravasation. *Advanced Healthcare Materials*, *7*(9), 1701257.

Najafi, M., Farhood, B., & Mortezaee, K. (2019). Extracellular matrix (ECM) stiffness and degradation as cancer drivers. *Journal of Cellular Biochemistry*, *120*(3), 2782–2790. https://doi.org/10.1002/jcb.27681

Nazir, S. U., Kumar, R., Singh, A., Khan, A., Tanwar, P., Tripathi, R., Mehrotra, R., & Hussain, S. (2019). Breast cancer invasion and progression by MMP-9 through Ets-1 transcription factor. *Gene*, *711*, 143952.

Nguyen, D. X., Bos, P. D., & Massague, J. (2009). Metastasis: From dissemination to organ-specific colonization. *Nature Reviews Cancer*, *9*(4), 274–284. https://doi.org/10.1038/nrc2622

Osaki, T., Sivathanu, V., & Kamm, R. D. (2018). Vascularized microfluidic organ-chips for drug screening, disease models and tissue engineering. *Current Opinion in Biotechnology*, *52*, 116–123. https://doi.org/10.1016/j.copbio.2018.03.011

Owyong, M., Chou, J., van den Bijgaart, R. J., Kong, N., Efe, G., Maynard, C., Talmi-Frank, D., Solomonov, I., Koopman, C., Hadler-Olsen, E., Headley, M., Lin, C., Wang, C. Y., Sagi, I., Werb, Z., & Plaks, V. (2019). MMP9 modulates the metastatic cascade and immune landscape for breast cancer anti-metastatic therapy. *Life Science Alliance*, *2*(6), e201800226.

Pandamooz, S., Jafari, A., Salehi, M. S., Jurek, B., Ahmadiani, A., Safari, A., Hassanajili, S., Borhani-Haghighi, A., Dianatpour, M., Niknejad, H., Azarpira, N., & Dargahi, L. (2020). Substrate stiffness affects the morphology and gene expression of epidermal neural crest stem cells in a short term culture. *Biotechnology and Bioengineering*, *117*(2), 305–317.

Paul, C. D., Mistriotis, P., & Konstantopoulos, K. (2017). Cancer cell motility: Lessons from migration in confined spaces. *Nature Reviews Cancer*, *17*(2), 131–140. https://doi.org/10.1038/nrc.2016.123

Piao, J., You, K., Guo, Y., Zhang, Y., Li, Z., & Geng, L. (2017). Substrate stiffness affects epithelial-mesenchymal transition of cervical cancer

cells through miR-106b and its target protein DAB2. *International Journal of Oncology*, *50*(6), 2033–2042.

Polacheck, W. J., German, A. E., Mammoto, A., Ingber, D. E., & Kamm, R. D. (2014). Mechanotransduction of fluid stresses governs 3D cell migration. *Proceedings of the National Academy of Sciences of the United States of America*, *111*(7), 2447–2452. https://doi.org/10.1073/pnas.1316848111

Ray, A., Slama, Z. M., Morford, R. K., Madden, S. A., & Provenzano, P. P. (2017). Enhanced directional migration of cancer stem cells in 3D aligned collagen matrices. *Biophysical Journal*, *112*(5), 1023–1036. https://doi.org/10.1016/j.bpj.2017.01.007

Rianna, C., & Radmacher, M. J. N. (2017). Influence of microenvironment topography and stiffness on the mechanics and motility of normal and cancer renal cells. *Nanoscale*, *9*(31), 11222–11230.

Rice, A., Cortes, E., Lachowski, D., Cheung, B., Karim, S., Morton, J., & Del Rio Hernandez, A. (2017). Matrix stiffness induces epithelial–mesenchymal transition and promotes chemoresistance in pancreatic cancer cells. *Oncogenesis*, *6*(7), e352.

Rueden, C. T., Schindelin, J., Hiner, M. C., DeZonia, B. E., Walter, A. E., Arena, E. T., & Eliceiri, K. W. (2017). ImageJ2: ImageJ for the next generation of scientific image data. *BMC Bioinformatics*, *18*(1), 529.

Shukla, V., Higuita-Castro, N., Nana-Sinkam, P., & Ghadiali, S. N. (2016). Substrate stiffness modulates lung cancer cell migration but not epithelial to mesenchymal transition. *Journal of Biomedical Materials Research, Part A*, *104*(5), 1182–1193.

Sleeboom, J. J. F., Eslami Amirabadi, H., Nair, P., Sahlgren, C. M., & den Toonder, J. M. J. (2018). Metastasis in context: Modeling the tumor microenvironment with cancer-on-a-chip approaches. *Disease Models & Mechanisms*, *11*(3), dmm033100. https://doi.org/10.1242/dmm.033100

Sokeland, G., & Schumacher, U. (2019). The functional role of integrins during intra- and extravasation within the metastatic cascade. *Molecular Cancer*, *18*(1), 12. https://doi.org/10.1186/s12943-018-0937-3

Staunton, J. R., Vieira, W., Fung, K. L., Lake, R., Devine, A., & Tanner, K. (2016). Mechanical properties of the tumor stromal microenvironment probed in vitro and ex vivo by in situ-calibrated optical trap-based active microrheology. *Cellular and Molecular Bioengineering*, *9*(3), 398–417.

Stuelten, C. H., Parent, C. A., & Montell, D. J. (2018). Cell motility in cancer invasion and metastasis: Insights from simple model organisms. *Nature Reviews Cancer*, *18*(5), 296–312. https://doi.org/10.1038/nrc.2018.15

Vickerman, V., & Kamm, R. D. (2012). Mechanism of a flow-gated angiogenesis switch: Early signaling events at cell–matrix and cell–cell junctions. *Integrative Biology*, *4*(8), 863–874.

Walker, C., Mojares, E., & Del Rio Hernandez, A. (2018). Role of extracellular matrix in development and cancer progression. *International Journal of Molecular Sciences*, *19*(10), 3028. https://doi.org/10.3390/ijms19103028

White, K. A., Grillo-Hill, B. K., & Barber, D. L. (2017). Cancer cell behaviors mediated by dysregulated pH dynamics at a glance. *Journal of Cell Science*, *130*(4), 663–669. https://doi.org/10.1242/jcs.195297

Wolf, K., Te Lindert, M., Krause, M., Alexander, S., te Riet, J., Willis, A. L., Hoffman, R. M., Figdor, C. G., Weiss, S. J., & Friedl, P. (2013). Physical limits of cell migration: Control by ECM space and nuclear deformation and tuning by proteolysis and traction force. *Journal of Cell Biology*, *201*(7), 1069–1084. https://doi.org/10.1083/jcb.201210152

Wullkopf, L., West, A.-K. V., Leijnse, N., Cox, T. R., Madsen, C. D., Oddershede, L. B., & Erler, J. T. (2018). Cancer cells' ability to mechanically adjust to extracellular matrix stiffness correlates with their invasive potential. *Molecular Biology of the Cell*, *29*(20), 2378–2385.

Xu, Z., Li, E., Guo, Z., Yu, R., Hao, H., Xu, Y., Sun, Z., Li, X., Lyu, J., & Wang, Q. (2016). Design and construction of a multi-organ microfluidic chip mimicking the in vivo microenvironment of lung cancer metastasis. *ACS Applied Materials & Interfaces*, *8*(39), 25840–25847. https://doi.org/10.1021/acsami.6b08746

Zervantonakis, I. K., Hughes-Alford, S. K., Charest, J. L., Condeelis, J. S., Gertler, F. B., & Kamm, R. D. (2012). Three-dimensional microfluidic model for tumor cell intravasation and endothelial barrier function. *Proceedings of the National Academy of Sciences of the United States of America*, *109*(34), 13515–13520. https://doi.org/10.1073/pnas.1210182109

Zhang, Q., Liu, T., & Qin, J. (2012). A microfluidic-based device for study of transendothelial invasion of tumor aggregates in realtime. *Lab on a Chip*, *12*(16), 2837–2842. https://doi.org/10.1039/c2lc00030j

Zhao, D., Li, Q., Liu, M., Ma, W., Zhou, T., Xue, C., & Cai, X. (2018). Substrate stiffness regulated migration and invasion ability of adenoid cystic carcinoma cells via RhoA/ROCK pathway. *Cell Proliferation*, *51*(3), e12442. https://doi.org/10.1111/cpr.12442

Zhao, D., Xue, C., Li, Q., Liu, M., Ma, W., Zhou, T., & Lin, Y. (2018). Substrate stiffness regulated migration and angiogenesis potential of A549 cells and HUVECs. *Journal of Cellular Physiology*, *233*(4), 3407–3417. https://doi.org/10.1002/jcp.26189

How to cite this article: Azadi S, Tafazzoli Shadpour M, Warkiani ME. Characterizing the effect of substrate stiffness on the extravasation potential of breast cancer cells using a 3D microfluidic model. *Biotechnology and Bioengineering*. 2021;118:823–835. https://doi.org/10.1002/bit.27612